Tensor-product elliptic solver for liquid-metal magnetohydrodynamics

Leibniz Rechenzentrum Garching

SuperMUC-NG Status and Results Workshop, May 9 – 11, 2023

Computing project: **pn68ni**

Project PI: Prof. Jörg Schumacher (TU Ilmenau)

Contributors: D. Krasnov[1], P. Vieweg[1], Yu. Kolesnikov[1], K.R. Sreenivasan[2], A. Pandey[2], O. Zikanov[3], Ya. Listratov[4], I. Belyaev[4], Sh. Bhattacharya[1], T. Boeck[1],

Research network

TECHNISCHE UNIVERSITÄT ILMENAU

TU Ilmenau[(1)]

New York University, NYU Abu-Dhabi[(2)]

University of Michigan Dearborn[(3)]

MPEI, JIHT-RAS[(4)] (Moscow)

Research topics covered in 2022-2023

1. Turbulent convection at very low Prandtl numbers
2. Development of numerical tools for wall-bounded MHD flows
3. Evolution of MHD flows in ducts and rectangular boxes

Applications:

Solar convection with $Pr \sim 10^{-6}$

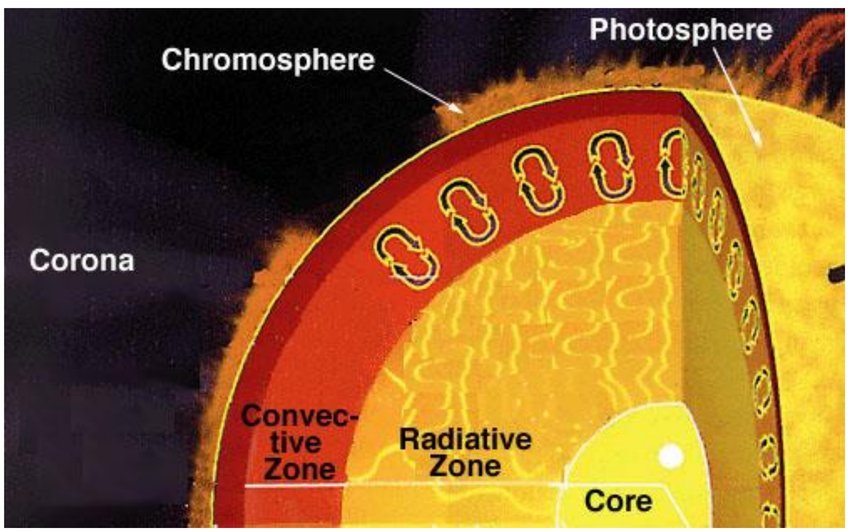

https://eng.libretexts.org/@go/page/5948?pdf

Liquid-metal cooling blankets with $Pr \sim 10^{-2}$ for fusion reactors (iter.org)

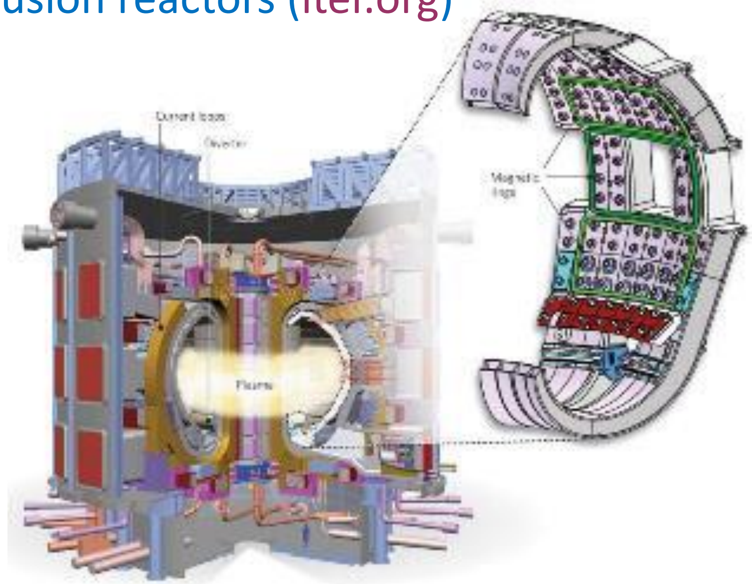

Tools applied

1. In-house flow solver for incompressible flows in rectangular geometries (TU Ilmenau, UMICH Dearborn)

*Key features: based on 2nd order finite-differences, conservative scheme, structured collocated grids, MPI + Open MP hybrid parallelization

2. NEK 5000 solver, open-source community driven code (TU Ilmenau, NYU, NYU Abu-Dhabi)

*Key features: spatial discretization with spectral elements, unstructured grids, multi-domain decomposition, MPI parallelization

3. Experimental facilities with liquid mercury (Moscow)

*Solenoid magnet up to 1.7T, temperature probes, electric potential sensors

Physical model:

- ***Governing equations:***

$$\nabla \cdot \boldsymbol{u} = 0$$

$$\frac{\partial \boldsymbol{u}}{\partial t} + (\boldsymbol{u} \cdot \nabla)\boldsymbol{u} = -\nabla p + \sqrt{\frac{Pr}{Ra}}[\nabla^2 \boldsymbol{u} + Ha^2(\boldsymbol{j} \times \boldsymbol{e_z})] + T\boldsymbol{e_z}$$

$$\frac{\partial T}{\partial t} + (\boldsymbol{u} \cdot \nabla)T = \sqrt{\frac{1}{RaPr}}\nabla^2 T$$

$$\boldsymbol{j} = -\nabla \varphi + (\boldsymbol{u} \times \boldsymbol{e_z})$$

$$\nabla^2 \varphi = \nabla \cdot (\boldsymbol{u} \times \boldsymbol{e_z})$$

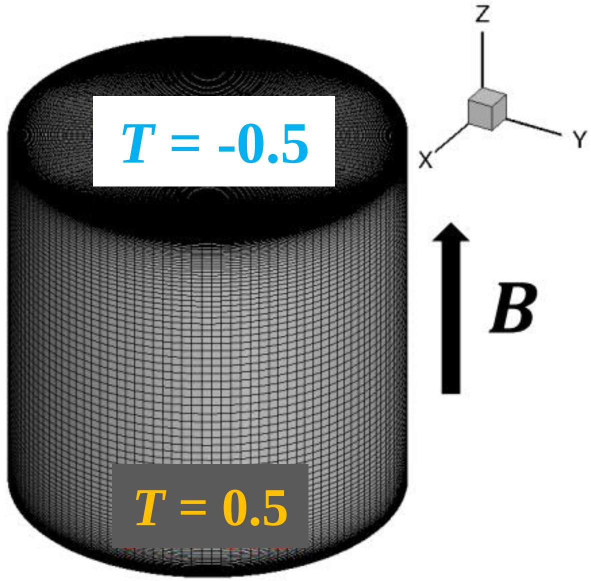

- lateral walls are thermally insulated
- all walls are perfectly electrically insulated

Not anymore !!!

- ***Approximations:***
  - The Boussinesq approximation
  - The quasi-static model of electromagnetic interactions: $Re_m << 1$ and $Pr_m << 1$

- ***Non-dimensional control parameters:***

$$Pr = \frac{\nu}{\kappa} \qquad Ra = \frac{g\alpha\Delta T H^3}{\nu\kappa} \qquad Ha = B_o H\sqrt{\frac{\sigma}{\rho\nu}} \qquad \Gamma = \frac{D}{H}$$

#1: Turbulent convection at low Prandtl numbers

Parameters of simulations with FD in-house solver

rectangular box with aspect ratio L/H = 25/1 (width/height)

Ra = 10^5 … 10^7 and *Pr* = 0.021, 0.005, 0.001

Simulation	Resolution	Computing information	*Nu*	*Re*
Ra = 1e6, *Pr* = 0.021	8192^2 x 512	34 Bill. points, @ 24576 cores	4.74282523	3155
Ra = 1e6, *Pr* = 0.005	8192^2 x 512	34 Bill. points, @ 24576 cores	3.48979662	7638
Ra = 1e6, *Pr* = 0.001	12800^2 x 800	131 Bill. points, @ 38400 cores	2.47784979	19901
Ra = 1e5, *Pr* = 0.001	9600^2 x 640	60 Bill. points, @ 28800 cores	1.21289961	4776
Ra = 1e7, *Pr* = 0.001	20480^2 x 1280	0.54 Trill. points, @ 144000 cores	4.60336402	56103

Information about the largest simulation at *Ra* = 10^7 and *Pr* = 10^{-3}

(*) consumed compute time totals 35 Mill. core-hours (one run at 144000 cores)

(*) highest resolution maxed out at 22400^2 x 1400 = 0.7 Trill. points

(*) one snapshot with 3D flow field exceeds 17 TB

(*) total data to be post-processed more than 190 TB

#1: Turbulent convection at low Prandtl numbers

Flow field at *Ra = 10^5* and *Pr = 0.001* and Γ = 25 (L/H)

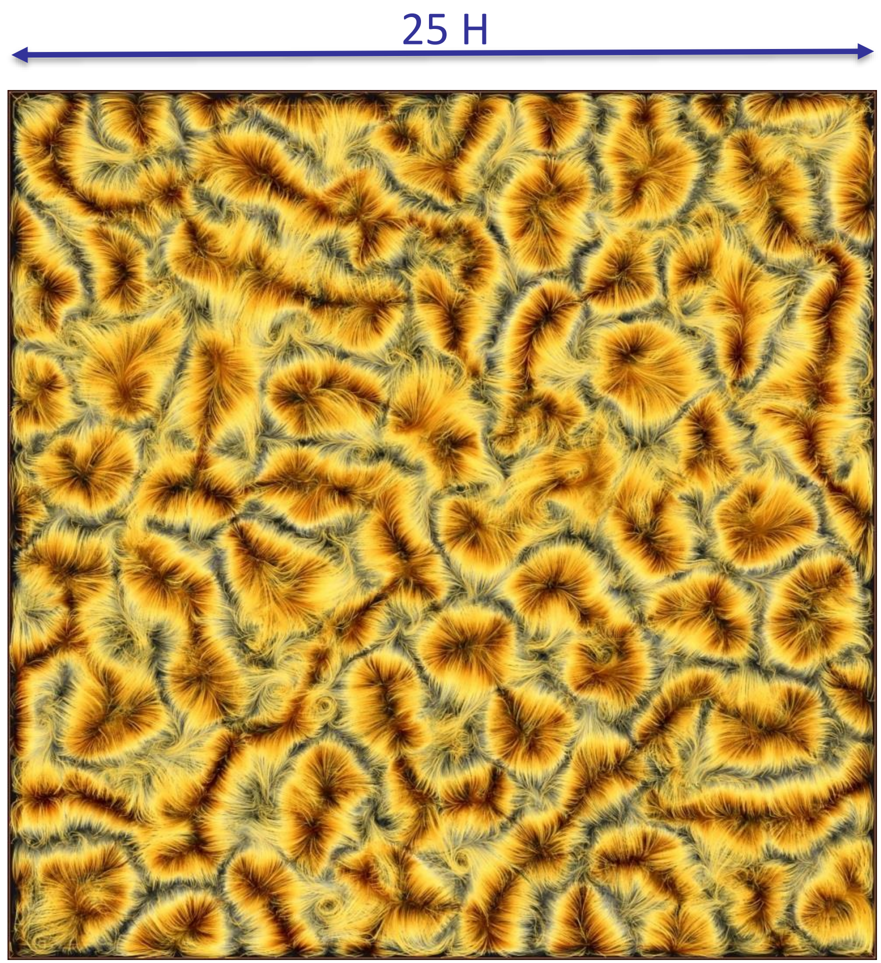

Superstructures shown by streamlines, seeded with 15000 lines

#1: Turbulent convection at low Prandtl numbers

Flow fields at *Pr = 0.001*

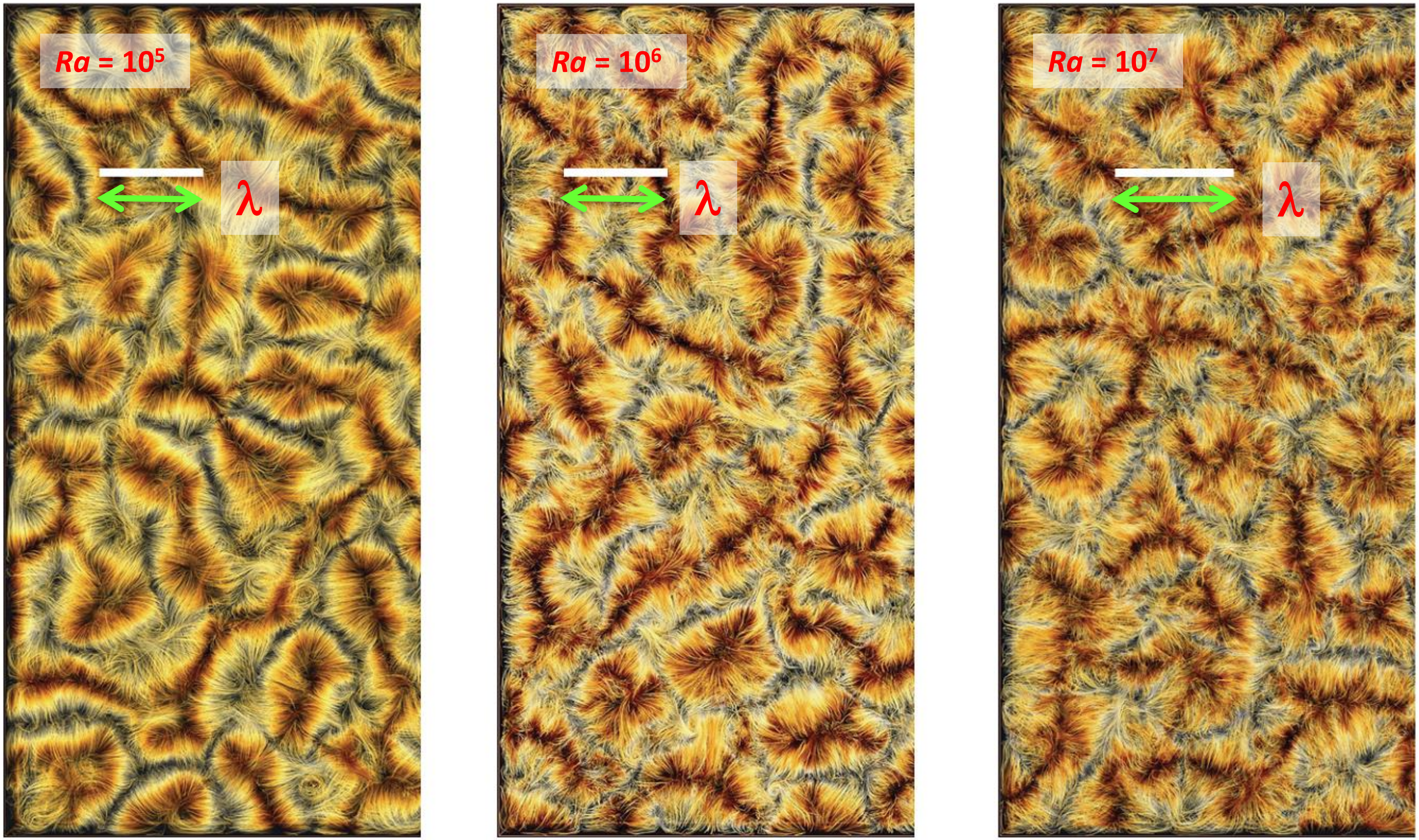

λ – characteristic length of superstructures as typical distance between two up- or down-welling regions, about ~ ***3H***

#1: Turbulent convection at low Prandtl numbers

Vertical velocity *Vz* in the mid-plane at *Ra = 10⁶* and *Pr = 0.001*

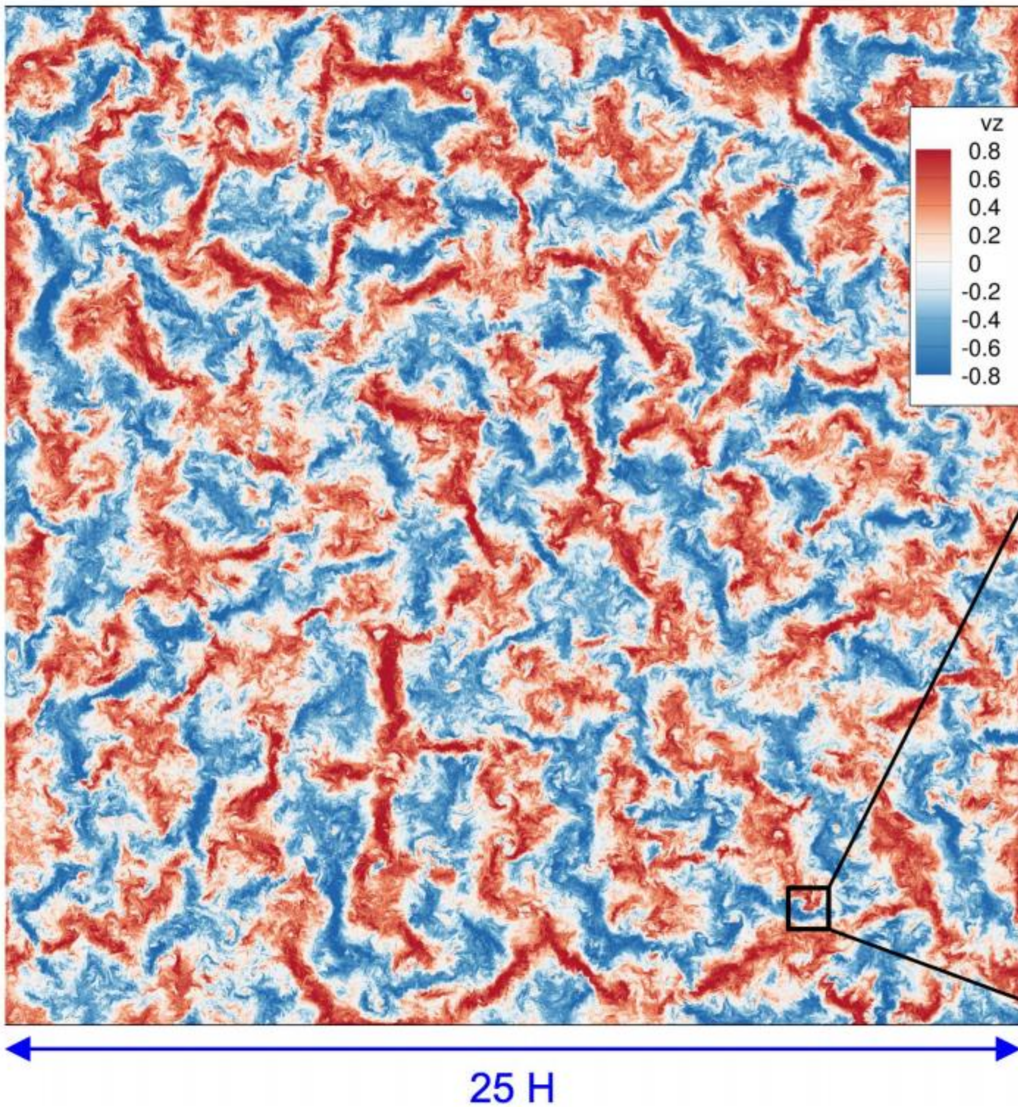

On the left – entire domain, visualized at full resolution of 12800 x 12800 pixels (i.e. one pixel = one grid point)

Zoom into a 1/1 region, displaying highly intertial small-scale turbulence

δ_T indicates thickness of the thermal boundary layer

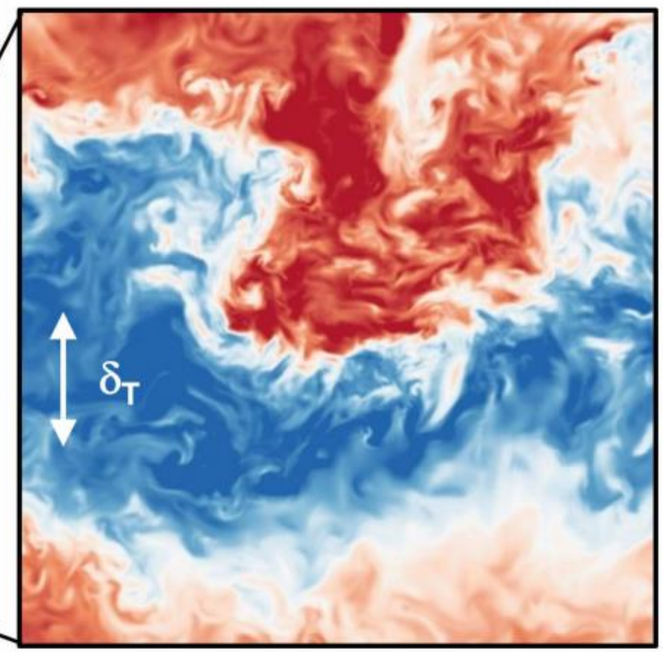

<u>Important finding</u>: Turbulence in the bulk is Kolmogorov-like with $E(k) \sim k^{-5/3}$

- Pandey et.al., J. Fluid. Mech. (2022)

Archetypal system: MHD flow in square duct

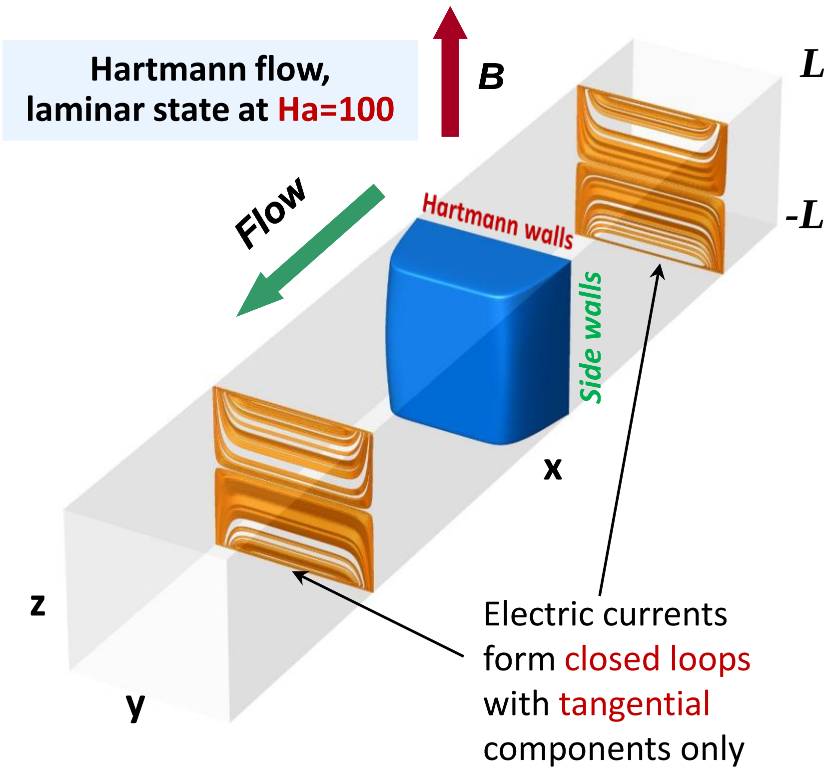

Hartmann case: all 4 walls are insulating

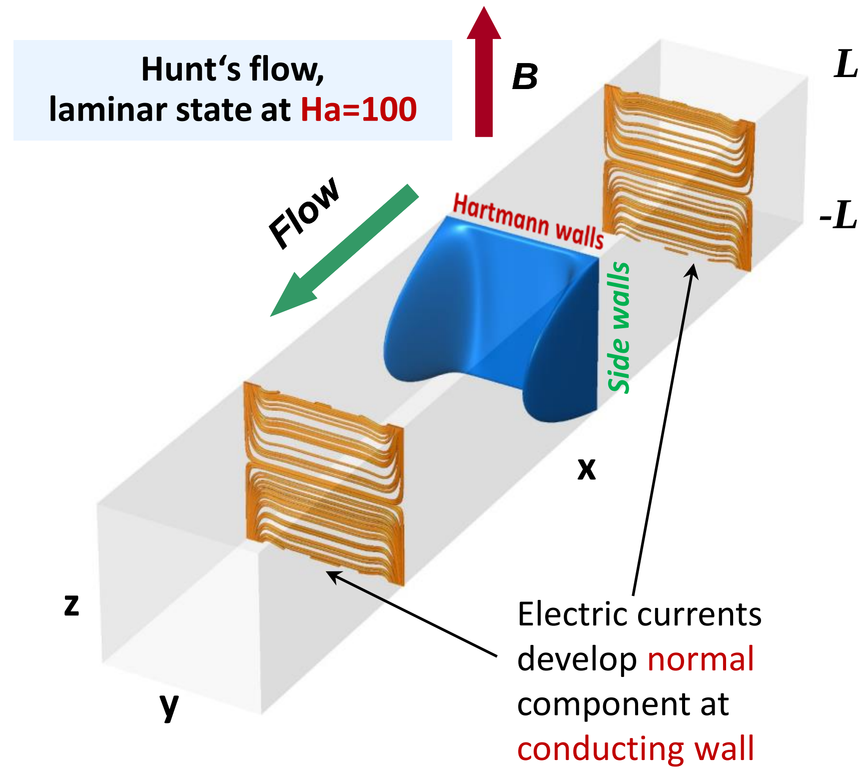

Hunt's case: conducting Hartmann walls, insulating sidewalls (Shercliff walls)

- Boundary condition for electric potential, idealized cases

Side wall	$\partial\varphi/\partial n = 0$	$\partial\varphi/\partial n = 0$
Hartmann wall	$\partial\varphi/\partial n = 0$	$\varphi = const$
	perfectly insulating	perfectly conducting

Finite-wall conductivity (realistic scenario)

Wall conductance ratio $C_w = \frac{\sigma_w \tau_w}{\sigma L}$

σ_w and τ_w – conductivity and thickness of the wall

σ and L – conductivity and thickness of the fluid layer

Case 1: *Ha* = 100 → Case 2: *Ha* = 1000

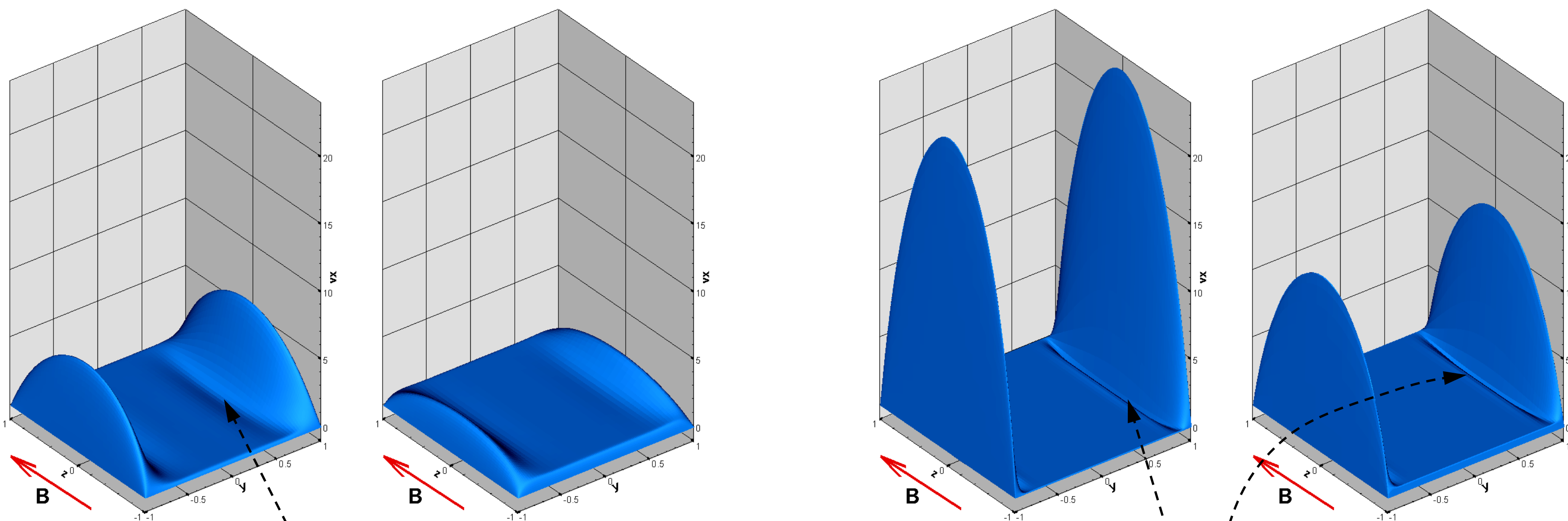

Ideally conducting Hartmann walls	Finite conductance ratio $C_w = 0.1$	Ideally conducting Hartmann walls	Finite conductance ratio $C_w = 0.1$

Importance: at high *Ha* the basic velocity profile develops inflection points in the region of side-jets – the flow, therefore, may (and do!) become unstable even at very low-*Re*

#2: Development of numerical tools for wall-bounded MHD flows

Tensor-product Elliptic solver for finite-wall conductivity

Classic boundary conditions

$$\nabla^2\phi = \nabla\cdot(\boldsymbol{u}\times\boldsymbol{e}_B)$$

Elliptic (Poisson) equation for electric potential ϕ

$$\frac{\partial\phi}{\partial n} = 0$$

Perfectly **insulating** wall (Neumann bc)

and/or

$$\phi = const$$

Perfectly **conducting** wall (Dirichlet bc)

Realistic boundary condition for thin-walls with finite conductivity

$$\left.\frac{\partial\phi}{\partial n}\right|_{wall} = C_w \nabla_\perp^2\phi\Big|_{wall}$$

Wall-normal derivative

Tangential 2D Laplace operator at the wall

$$C_w = \frac{\sigma_w \tau_w}{\sigma L}$$

Wall conductance ratio C_w

First proposed: J.S. Walker, J. Méc. (1981)

Main issue: solution depends on boundary conditions, whereas boundary conditions depend on solution – chicken and egg problem

Efficient and simple direct solution:

Tensor-product approach, based on identifying the eigenmodes expansion for tridiagonal matrices of discrete Laplace operator, modified by embedded thin-wall conditions

The approach can be applied on structured grids with arbitrary clustering/stretching

#2: Development of numerical tools for wall-bounded MHD flows

What is tensor-product approach for elliptic equations?

Tensor-product approach can be seen as the most generalized form of Fourier expansion, i.e. expansion into eigenmodes

$$\frac{\delta^2\phi}{\delta x^2}+\frac{\delta^2\phi}{\delta y^2}+\frac{\delta^2\phi}{\delta z^2}=r$$

Discrete 3D Poisson equation for ϕ

Each of these operators $\frac{\delta^2\varphi}{\delta x^2}, \frac{\delta^2\varphi}{\delta y^2}, \frac{\delta^2\varphi}{\delta z^2}$ can be represented as tridiagonal matrix for the 3-point stencils of 2nd derivative

$$\frac{\delta^2}{\delta x^2}=\frac{1}{h^2}\begin{bmatrix}-2 & \cdots & \cdots \\ 1 & -2 & 1 \\ \cdots & \cdots & -2\end{bmatrix}$$

Tridiag. matrix T_x for x-uniform grid

(1) Core idea – find eigenvalues λ, eigenvectors and inverse eigenvectors for tridiagonal matrices T_x and T_y corresponding to horizontal operators in **x-** and **y-**directions:

$T_x \to A$ (direct), λ_x and A^{-1} (inverse) and $T_y \to B$ (direct), λ_y and B^{-1} (inverse)

(2) 3D elliptic problem can be converted to the eigenmodes space as series of 1D problems amenable to fast Thomas tridiagonal solver in the remaining **z-**direction

$$\left(\lambda_{x,i}+\lambda_{y,j}+\frac{\delta^2}{\delta z^2}\right)\hat{\phi}_{i,j}(z)=\hat{r}_{i,j}(z),\ i=1,\ldots,N_x,\ j=1,\ldots,N_y$$

For uniform grids this approach retains full compatibility with fast transforms (FFT, cosFT, sinFT)!!!

The eigenvectors A, B converge to
- Fourier modes for periodic conditions
- Cosine modes for Neumann conditions
- Sine modes for Dirichlet conditions

The eigenvalues λ_x and λ_y become $-k_x^2$ and $-k_y^2$, i.e. negatives of the square of the wave-numbers

#2: Development of numerical tools for wall-bounded MHD flows

Embedding thin-wall b.c. into eigenmode expansion

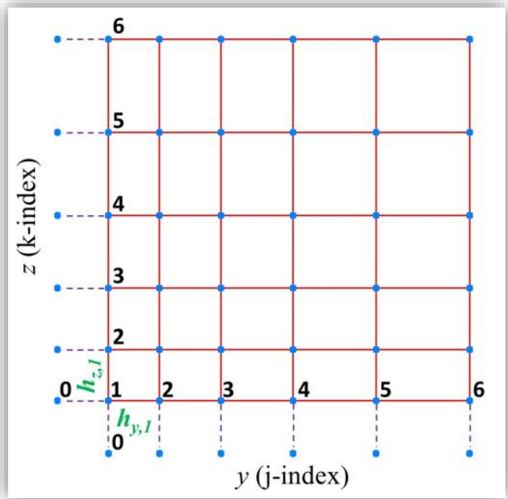

Example of rectangular grid in (y,z)

$$\frac{\phi_2-\phi_0}{2h_1} = C_w\left(\frac{\delta^2\phi}{\delta x^2}+\frac{\delta^2\phi}{\delta y^2}\right)_{z_1}$$

Discrete thin-wall boundary condition

+

$$\frac{\delta^2\phi}{\delta x^2}+\frac{\delta^2\phi}{\delta y^2}+\frac{\delta^2\phi}{\delta z^2}=r$$

Discrete 3D Poisson equation

$$\frac{2\phi_2}{h_1^2}-\frac{2\phi_1}{h_1^2}+\left(1-\frac{2C_w}{h_1}\right)\left(\frac{\delta^2\phi}{\delta x^2}+\frac{\delta^2\phi}{\delta y^2}\right)_{z_1}=r_1$$

This form of thin-wall condition can be implemented with eigenmodes expansion

Two methods are possible, both amount to modification of the tridiagonal matrices

Method 1. Solving problem in transformed (eigenmodes) space, corner elements of the tridiag. matrix for Thomas solver are modified

$$\frac{2\hat{\phi}_2}{h_1^2}-\frac{2\hat{\phi}_1}{h_1^2}+\left(1-\frac{2C_w}{h_1}\right)(\lambda_{x,i}+\lambda_{y,j})\,\hat{\phi}_1=\hat{r}_1 \quad\Rightarrow\quad [a_1,b_1,c_1]=\left[\times,\,-\frac{2}{h_1^2}+\left(1-\frac{2C_w}{h_1}\right)(\lambda_{x,i}+\lambda_{y,j}),\,\frac{2}{h_1^2}\right]$$

Method 2. Modify tridiag. matrix in real space, then use this matrix to identify modified eigenmodes, then transform and solve

$$\frac{2\phi_2}{h_1^2}\frac{h_1}{h_1-2C_w}-\frac{2\phi_1}{h_1^2}\frac{h_1}{h_1-2C_w}+\left(\frac{\delta^2\phi}{\delta x^2}+\frac{\delta^2\phi}{\delta y^2}\right)_{z_1}=r_1\frac{h_1}{h_1-2C_w} \quad\Rightarrow\quad [a_1,b_1,c_1]=\left[\times,\,-\frac{2}{h_1^2}\frac{h_1}{h_1-2C_w},\,\frac{2}{h_1^2}\frac{h_1}{h_1-2C_w}\right]$$

#2: Development of numerical tools for wall-bounded MHD flows

Benchmarks of tensor-product vs. other methods
(performed on SuperMUC-NG)

Rayleigh-Bénard convection in a rectangular box computed on grids with various $N_x = N_y = N$ and $N_z = 256$
Clock time required to compute 100 time steps on 256 cores is shown as a function of N
Matrix multiplications in general TPT are performed with MKL multi-thread routines

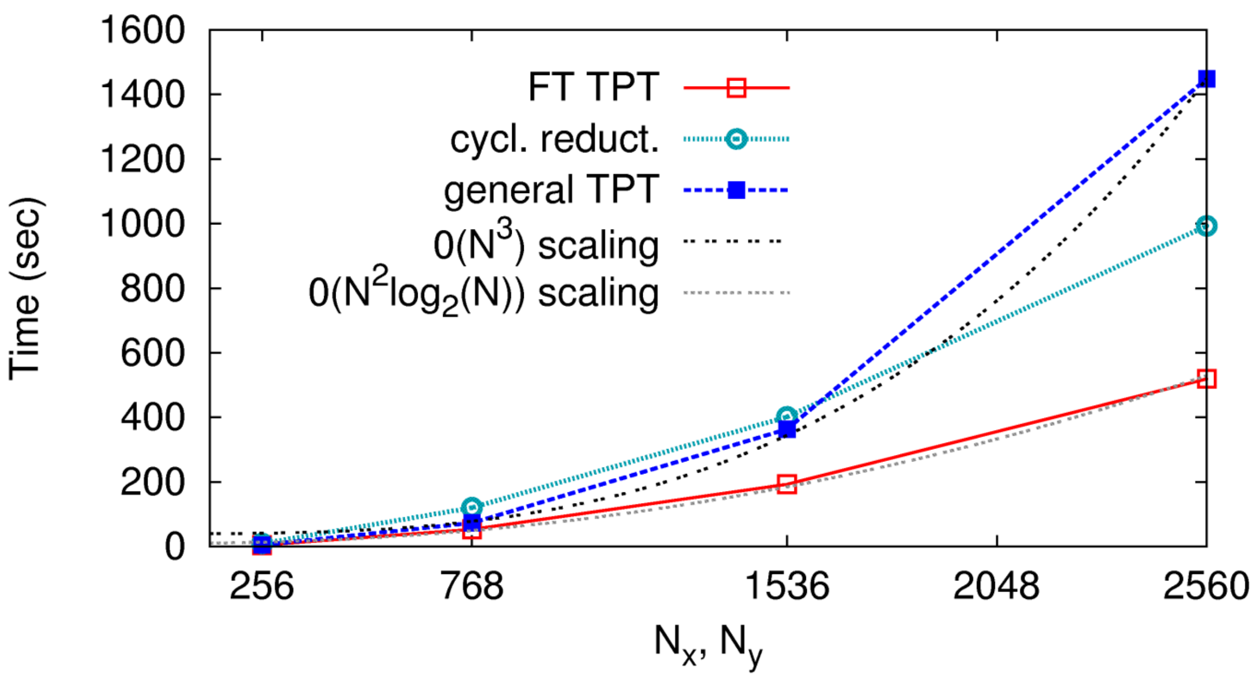

General TPT = Tensor-Product-Thomas solver, i.e. MatMul in x,y and Thomas method in z
Cycl. Reduct. = Cosine-FT in x and 2D Cyclic reduction method (Fishpack) in y,z
FT TPT = Fast Transform Tensor-Product-Thomas, i.e. Cosine-FT in x,y and Thomas method in z

→ Only TPT allows for arbitrary grid-clustering in x,y,z

#2: Tensor-product elliptic solver, list of pros and cons

(in part inspired by car reviews ☺ from Mat Watson/carwow youtube)

- Five good points about the car
- Five annoying points about the car

Copyright carwow.co.uk and Mat Watson

Prerequisite – elliptic problem should be separable, thus decomposition into eigenmodes can be applied
(basically that implies constant coefficients and structured grids)

Good points

- Direct solver – no iterations, no convergence issues
- Arbitrary grid-clustering in all 3 directions
- MKL matmul routines scale up almost linearly vs. number of threads
- Can be extended to curvilinear grid if separable (e.g. cylinder coords.)
- No speed-penalty vs. classic Neumann and Dirichet conditions
- Each wall can be assigned its own conductance ratio C_w
- Can be applied for finite thermal conductivity, even for unsteady form

Annoying points

- Transform matrices grow in size as n^2 – potential issue at hi-res
- Matrix multiplication scales as $O(n^3)$, vs. $O(n^2\log_2(n))$ for FFT/CosFT/SinFT

#3: Evolution of MHD flows in ducts and rectangular boxes (examples)

MHD flows in ducts with conducting walls – typical configuration for liquid-metal fusion blankets
Spatial evolution of Hunt's flow at Re = 2000, Ha = 2000 and C_w = 0.03

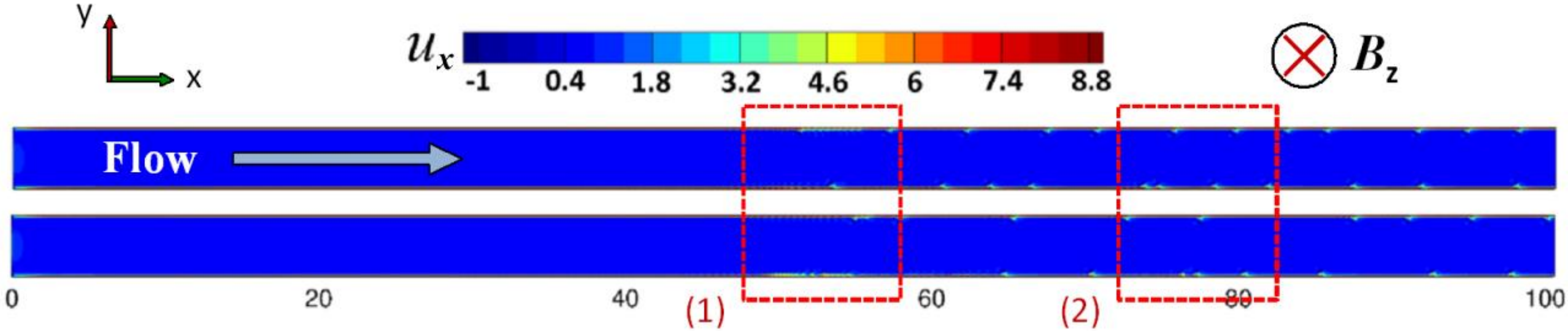

Region (1): Onset of sidewall jet instabilities

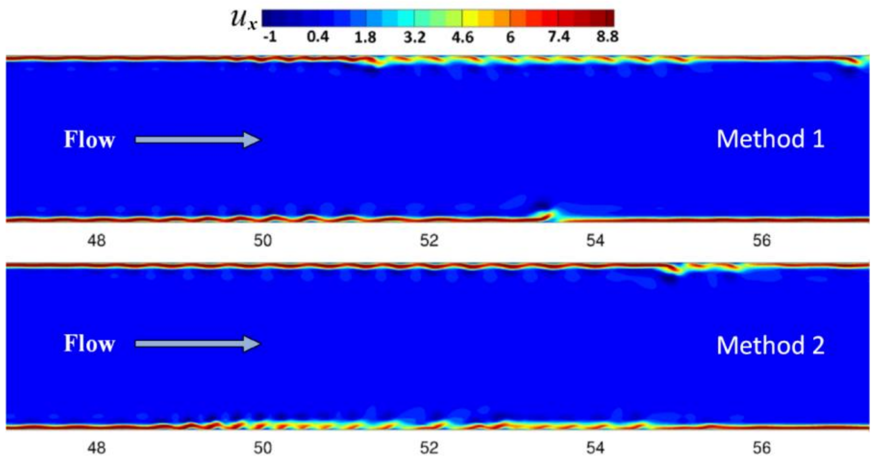

Region (2): Fully developed jet detachments

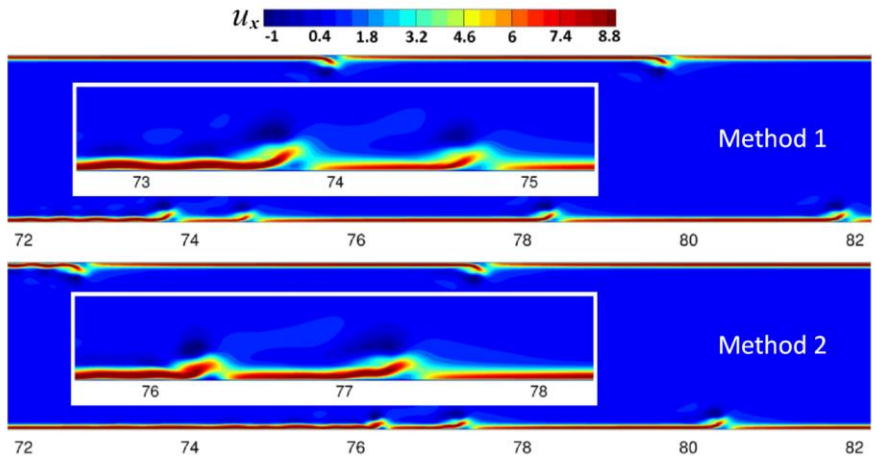

- Krasnov et.al. J. Comp. Phys. (2023)

#3: Evolution of MHD flows in ducts and rectangular boxes (examples)

Effect of wall conductivity on instability of a submerged round jet, entering square duct
Uniform vertical magnetic field B_z at *Ha*=500, flow at *Re*=1000

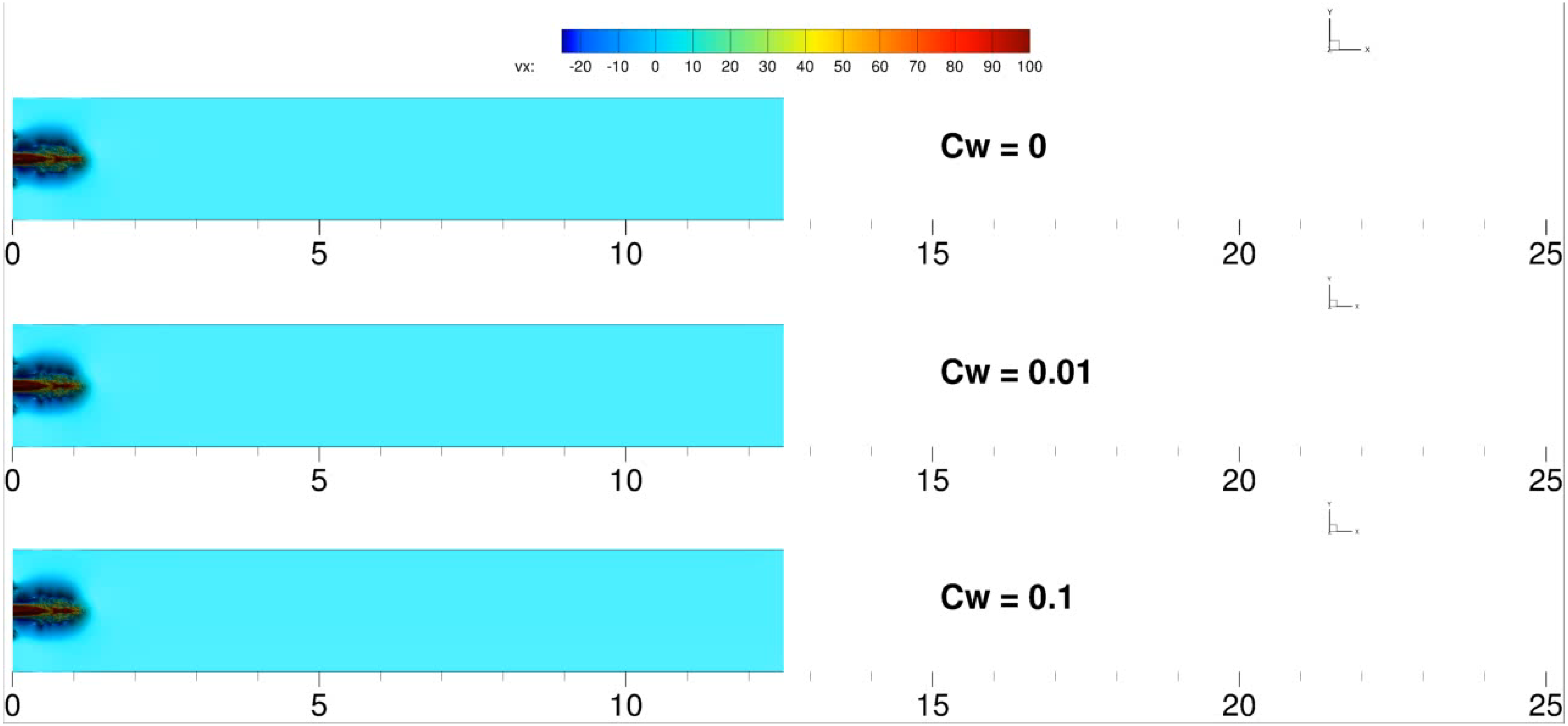

- Belyaev et.al., J. Fluid. Mech. (2023)

#3: Evolution of MHD flows in ducts and rectangular boxes (examples)

Magneto-thermal convection flows around and above the Chandrasekhar stability limit
At these conditions convective motion is expected to be fully suppressed by strong magnetic field
However, residual motion at the sidewalls – wall-modes – can exist far above even if the rest has "died"

<u>Fundamental</u>: effect of wall conductivity on the wall-modes at <u>uniform</u> magnetic field

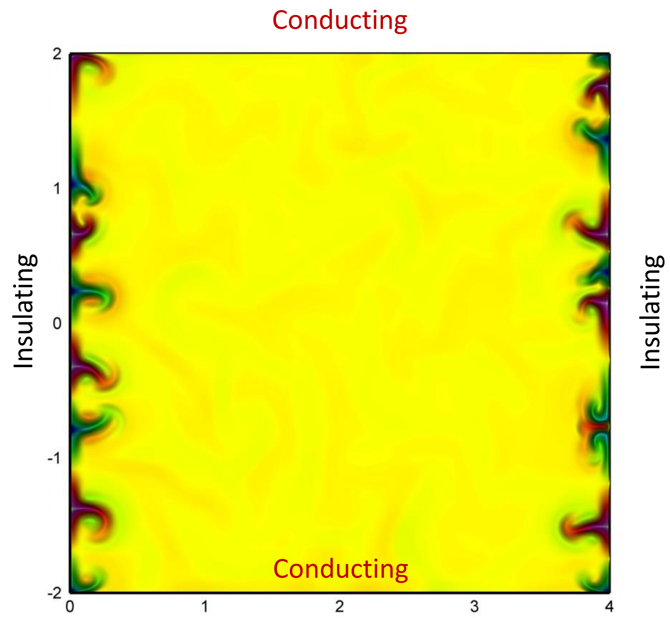

MHD convection in a rectangular box at Ra=10^7 and Ha=1000
Wall-modes are killed at conducting side-walls C_w=0.1

<u>Fusion relevant</u>: wall-modes at <u>fringing</u> magnetic field

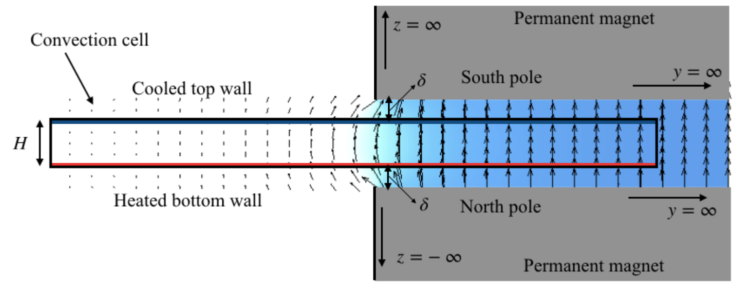

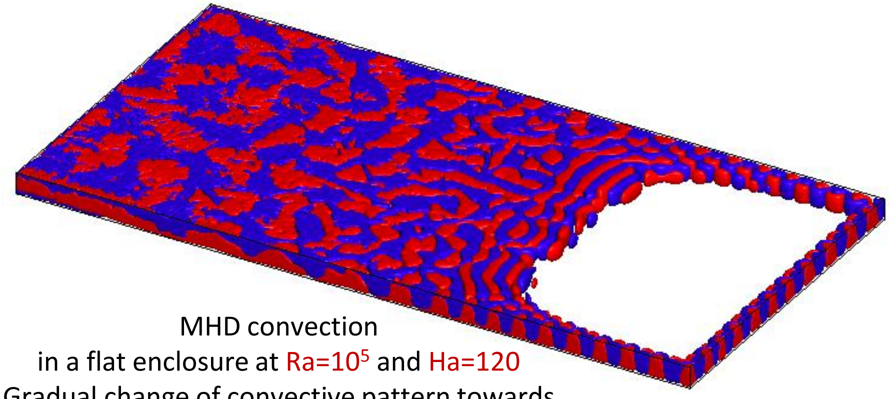

MHD convection
in a flat enclosure at Ra=10^5 and Ha=120
Gradual change of convective pattern towards anisotropic structures and wall-modes

- Bhattacharya et.al., J. Fluid Mech. (2023)

References

- A. Pandey, D. Krasnov, K. R. Sreenivasan and J. Schumacher, *Convective mesoscale turbulence at very low Prandtl numbers*, J. Fluid Mech. vol. 948, A23, 2022
- A. Pandey, D. Krasnov, J. Schumacher, R. Samtaney, K. R. Sreenivasan, *Similarities between characteristics of convective turbulence in confined and extended domains*, Physica D. 422, 2022
- *High Performance Computing in Science and Engineering*, LRZ Garching/Munich 2022
- I.A. Belyaev, I.S. Mironov, N.A. Luchinkin, Ya.I. Listratov, Yu. Kolesnikov, D. Kransov, O. Zikanov and S. Molokov, *Experimental study of submerged liquid metal jet in a rectangular duct in a transverse magnetic field*, J. Fluid Mech., 2023 (in press)
- D. Krasnov, A. Akhtari, O. Zikanov, J. Schumacher, Tensor-product-Thomas elliptic solver for liquid-metal magnetohydrodynamics, J. Comp. Phys. Vol. 474, 2023
- S. Bhattacharya, T. Boeck, D. Krasnov and J. Schumacher, *Effects of strong fringing magnetic fields on turbulent thermal convection,* J. Fluid Mech. 2023 (just accepted)

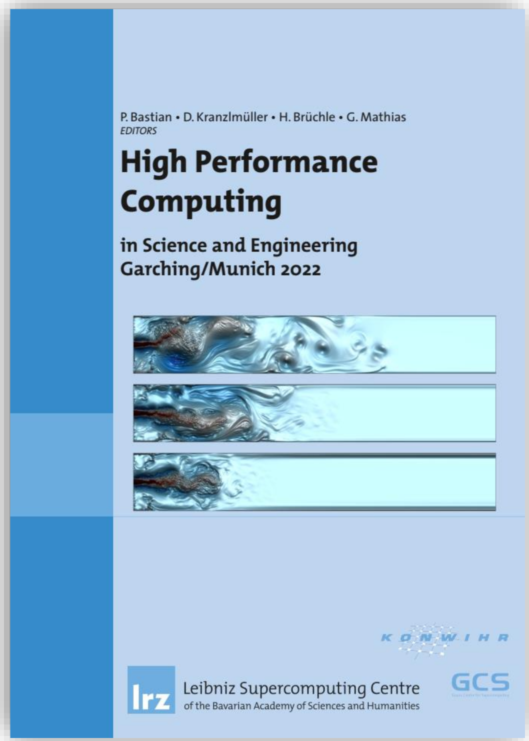

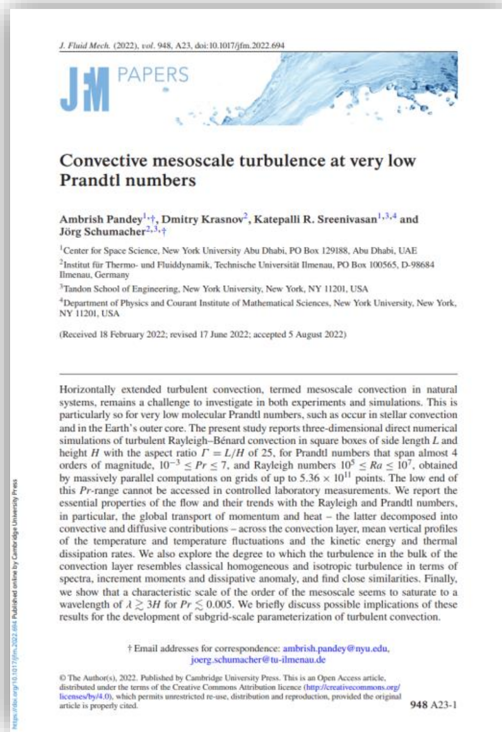
J. Fluid Mech. (2022), vol. 948, A23, doi:10.1017/jfm.2022.694

JFM PAPERS

Convective mesoscale turbulence at very low Prandtl numbers

Ambrish Pandey, Dmitry Krasnov, Katepalli R. Sreenivasan and Jörg Schumacher

948 A23-1


Journal of Computational Physics 474 (2023) 111784

Journal of Computational Physics

ELSEVIER

Tensor-product-Thomas elliptic solver for liquid-metal magnetohydrodynamics

Dmitry Krasnov, Ali Akhtari, Oleg Zikanov, Jörg Schumacher

ARTICLE INFO

ABSTRACT

1. Introduction

Outlook & Possible next steps

- Convection at low *Pr*: exploring broader parameter space and longer statistics (time-evolution)
- Extension of the tensor-product approach to solve problems with finite *thermal* wall-conductivity → conjugate heat transport "made easy"
- It would be interesting to explore application of practical algorithms of fast matrix multiplication possibly utilizing the symmetry properties of the transform matrices to achieve scaling better than $O(n^3)$

Thanks a lot for your attention!

Project support/Acknowledgements

DFG
Deutsche Forschungsgemeinschaft

NSF
National Science Foundation

Alexander von HUMBOLDT STIFTUNG

lrz
Leibniz-Rechenzentrum

GCS
Gauss Centre for Supercomputing